

# Equivalent Intrinsic Noise, Sampling Efficiency, and Contrast Sensitivity in Patients With Retinitis Pigmentosa

J. Jason McAnany,<sup>1</sup> Kenneth R. Alexander,<sup>1</sup> Mohamed A. Genead,<sup>2</sup> and Gerald A. Fishman<sup>1,2</sup>

<sup>1</sup>Department of Ophthalmology and Visual Sciences, University of Illinois at Chicago, Chicago, Illinois

<sup>2</sup>The Pangere Center for Inherited Retinal Diseases, The Chicago Lighthouse for People Who Are Blind or Visually Impaired, Chicago, Illinois

Correspondence: J. Jason McAnany, University of Illinois at Chicago, Department of Ophthalmology and Visual Sciences, 1855 W. Taylor Street, MC/648, Chicago, IL 60612; jmcana1@uic.edu.

Submitted: January 31, 2013

Accepted: May 2, 2013

Citation: McAnany JJ, Alexander KR, Genead MA, Fishman GA. Equivalent intrinsic noise, sampling efficiency, and contrast sensitivity in patients with retinitis pigmentosa. *Invest Ophthalmol Vis Sci.* 2013;54:3857-3862. DOI:10.1167/iovs.13-11789

**PURPOSE.** To determine the relationships among equivalent intrinsic noise ( $N_{eq}$ ), sampling efficiency, and contrast sensitivity (CS) in patients with retinitis pigmentosa (RP), where  $N_{eq}$  is an estimate of the amount of noise within the visual pathway and sampling efficiency represents the subject's ability to use stimulus information optimally.

**METHODS.** Participants included 10 patients with RP aged 10 to 54 years, who had visual acuities of 20/40 or better, and 10 visually normal control subjects aged 22 to 65 years. CS was measured for 2-cycles-per-degree Gabor patch targets presented in the absence of noise ( $CS_0$ ) and in five levels of noise spectral density. Data were fit with a standard linear amplifier model, which provided estimates of  $N_{eq}$  and sampling efficiency.

**RESULTS.**  $CS_0$  for the patients ranged from normal to as much as a factor of 3 below the lower limit of normal. All 10 patients had abnormally high  $N_{eq}$ , including two patients with normal  $CS_0$ . In comparison, only two patients had lower-than-normal sampling efficiency, and these two patients also had below-normal  $CS_0$ . Log  $CS_0$  for the patients was correlated significantly with log  $N_{eq}$  ( $r = -0.80$ ,  $P < 0.05$ ), but not with log efficiency ( $r = 0.54$ ,  $P = 0.11$ ).

**CONCLUSIONS.** Low CS was associated with elevated intrinsic noise in this group of RP patients, but even patients with normal CS had elevated noise levels. The results suggest that CS measurement in both the presence and absence of luminance noise can provide important information about visual dysfunction in RP patients.

Keywords: visual noise, contrast sensitivity, retinitis pigmentosa

Retinitis pigmentosa (RP) refers to a heterogeneous group of inherited retinal diseases characterized functionally by night blindness, visual field restrictions, and abnormalities in the electroretinogram.<sup>1</sup> The functional abnormalities are typically most pronounced in the peripheral visual field, but foveal function can also be affected, manifested clinically as a reduction in visual acuity.<sup>2-4</sup> Additionally, patients with RP can have low foveal contrast sensitivity (CS),<sup>5-7</sup> which is typically correlated significantly with their visual acuity<sup>8,9</sup> and visual field areas.<sup>8</sup>

A number of potential explanations for the deficits in foveal function in RP patients have been investigated and discounted, including a reduced quantal catch (the "dark glasses" model), spatial sampling irregularities due to photoreceptor dropout, and elevated intrinsic blur due to a loss of high spatial frequency analyzers.<sup>7,10,11</sup> A possible explanation for the low foveal CS in patients with RP that has not yet been evaluated is an abnormally high level of noise within the visual system. It has been proposed, for example, that most retinal diseases impair visual function by increasing the level of noise within the visual pathway.<sup>12</sup> Nevertheless, a study of four patients with age-related macular degeneration who had low CS found that only one patient had an abnormally high level of internal noise.<sup>13</sup> Therefore, the extent to which elevated internal noise accounts for the abnormal CS of RP patients remains unclear.

The amount of noise within the visual pathway can be evaluated using the "equivalent input noise method." Accord-

ing to this approach, CS measurements are made in the presence and absence of additive white luminance noise. The data are then analyzed within the context of a model of human performance in noise. A commonly used model is the linear amplifier model (LAM), which factors performance into two independent components: (1) equivalent intrinsic noise, which is an estimate of the amount of noise within the visual pathway; and (2) sampling efficiency, which represents the subject's ability to make use of stimulus information relative to an ideal observer.<sup>14</sup> The present study used the equivalent input noise approach and the LAM to investigate the relationships among equivalent intrinsic noise, sampling efficiency, and CS in patients with RP.

## METHODS

### Subjects

Ten patients with RP (three males and seven females, aged 10-54 years) participated in the study. No patient had an atrophic-appearing macular lesion or more than a minimal cataract in the tested eye, based on clinical examination. The Table gives the patients' ages, inheritance patterns, logarithm of the minimum angle of resolution (logMAR) visual acuities, Pelli-Robson letter contrast sensitivities, and horizontal diameters of the visual field (VF) obtained with a Goldmann II/4e target. The characteristics given in the Table are for the tested eye, which

TABLE. Subject Characteristics

Patient No.	Symbol	Age	RP Type	VA, logMAR	P-R CS	VF, deg
1	◆	30	ISO	-0.08	1.65	75
2	●	34	ISO	-0.04	1.65	30
3	▼	10	AR	0.00	1.65	70
4	▶	42	AD	0.00	1.65	70
5	◆	54	ISO	0.08	1.80	NA
6	○	13	USH2	0.10	1.95	40
7	▶	36	ISO	0.10	1.80	30
8	●	26	AR	0.18	1.65	0
9	■	23	AD	0.30	1.65	10
10	▲	24	AR	0.30	1.50	0
Control range	■	22 to 65		-0.17 to 0.04	1.95 to 1.65	

AD, autosomal dominant; AR, autosomal recessive; ISO, isolated; USH2, Usher syndrome type II; VA, visual acuity; P-R CS, Pelli-Robson letter contrast sensitivity; VF, visual field horizontal width using a Goldmann II/4e target.

was selected at random, but the fellow eye had similar characteristics. VF diameter was correlated significantly with logMAR visual acuity ( $r = -0.84$ ,  $P < 0.05$ ), consistent with previous research,<sup>8</sup> but there was no significant correlation between VF diameter and Pelli-Robson letter contrast sensitivity ( $r = 0.19$ ,  $P = 0.63$ ). By optical coherence tomography (OCT), six patients had a normal macula, two patients (nos. 8 and 10) had extrafoveal patchy losses of the inner segment ellipsoid region, and two patients (nos. 1 and 6) had slight extrafoveal microcystic changes, but none of the 10 patients had an epiretinal macular membrane.

Values of equivalent intrinsic noise and sampling efficiency from the patients with RP were compared with those of 10 visually normal control subjects, aged 22 to 65 years, who had best corrected visual acuities that were 0.04 logMAR or better and normal Pelli-Robson letter CS. The mean age of the control subjects was not significantly different from that of the patients ( $t = 1.03$ ,  $P = 0.32$ ). The study conformed to the tenets of the Declaration of Helsinki and the experiments were approved by an institutional review board at the University of Illinois at Chicago. Written informed consent was obtained from each subject prior to testing.

### Stimuli and Instrumentation

The instrumentation has been described in detail elsewhere.<sup>15</sup> In brief, stimuli were generated by a Macintosh G4 computer and were displayed on an NEC monitor (FE2111SB) with a screen resolution of  $1280 \times 1024$  and an 85-Hz refresh rate, driven by a video card with 10-bit digital to analog resolution (ATI Radeon 9000 Pro; Advanced Micro Devices, Sunnyvale, CA). The monitor, which was the only source of illumination in the room, was viewed monocularly through a phoropter with the subject's best refractive correction. A 3.0-mm artificial pupil mounted on the eyepiece of the phoropter was used to control the retinal illuminance. The luminance values of the display were derived from a linearized lookup table, which was calibrated with a photometer (Minolta LS 110; Konica Minolta, Tokyo, Japan). The temporal characteristics of the display were

confirmed using an oscilloscope and photocell. The experiments were written in a numerical computing environment (MATLAB; MathWorks, Natick, MA) using the Psychophysics Toolbox extensions.<sup>16</sup>

The test stimulus was a 2-cycle-per-degree Gabor patch (i.e., Gaussian-windowed sinusoidal grating), subtending  $1.7^\circ$ . Letter optotypes, which are broad-band in spatial frequency content, can complicate the interpretation of contrast sensitivity measurements,<sup>17</sup> so frequency-limited Gabor patch stimuli were used to ensure that the same spatial frequency information mediated contrast sensitivity for the patients and the controls at all levels of external noise. The Gabor patch was presented in sine phase either in the center of a uniform field with a luminance of  $50 \text{ cd/m}^2$  or in the center of a noise field of the same mean luminance. The contrast ( $C$ ) of the Gabor patch was defined as Weber contrast:

$$C = (L_P - L_M) / L_M \quad (1)$$

where  $L_P$  was the peak luminance of the Gabor patch in cosine phase and  $L_M$  was its mean luminance.

The noise field, which covered an area that was approximately 1.5 times larger than the Gabor patch, consisted of independently generated square checks with luminances drawn randomly from a uniform distribution. Each noise check subtended  $0.083^\circ$  by  $0.083^\circ$ , which corresponds to six noise checks per cycle of the Gabor patch, a value consistent with that used by others.<sup>12</sup> The check duration was 0.012 seconds (1 video frame). The noise spectral density ( $N$ ) ranged from 0 to  $1 \times 10^{-5} \text{ deg}^2/\text{s}$  in 0.5 log unit steps and was computed as the product of the noise check area, check duration, and the root mean square contrast of the noise check squared.<sup>18</sup>

As illustrated in Figure 1, the target duration was 106 ms and the total noise duration was 318 ms. The target onset was delayed relative to the noise onset by 106 ms and the duration of the noise that preceded the target was equal to the noise duration following the target offset. This type of asynchronous presentation is used commonly in studies of equivalent intrinsic noise.<sup>12,15,18-21</sup>

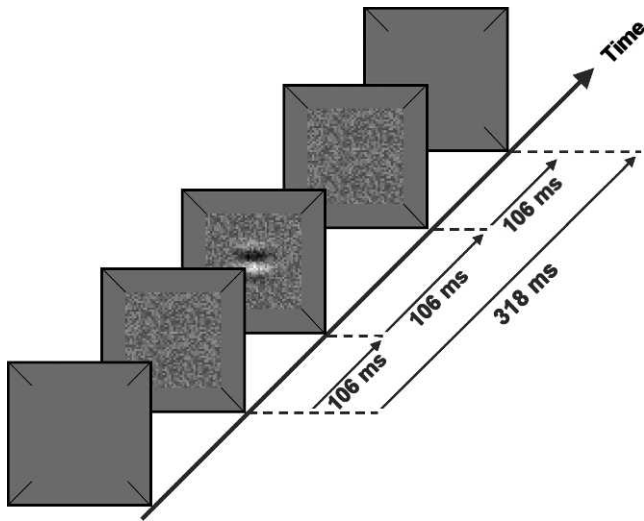


FIGURE 1. Schematic illustration of the temporal sequence of stimulus presentation in which a target of 106-ms duration was added to luminance noise of 318-ms total duration, with 106 ms of noise preceding and following the target presentation.

**Procedure**

Prior to all measurements, the pupil of the tested eye was dilated with 2.5% phenylephrine hydrochloride and the display was viewed through the 3-mm artificial pupil. A 30-second period of adaptation to a uniform field preceded each session, and a brief warning tone signaled the start of each stimulus presentation. The subject's task was to judge the orientation of the Gabor patch, which was randomly displayed either horizontally or vertically on each trial. No feedback was given. Contrast threshold was measured using the QUEST adaptive staircase procedure,<sup>22</sup> with 40 trials per condition and a targeted value of 82% correct. For each subject, contrast threshold was measured in the absence of noise and in the presence of each of the five external noise levels ( $N$ ) with the order of conditions randomized.

**Analysis**

Data were analyzed using the LAM as follows. First, contrast threshold measurements were converted to log threshold signal energy ( $E_t$ ), which was computed as the integral over space and time of the squared signal function.<sup>18</sup> Next,  $\log E_t$  was plotted as a function of  $\log N$  and the data were fit with the following equation<sup>14</sup>:

$$\log E_t = \log(k) + \log(N + N_{eq}) \tag{2}$$

where  $k$  and  $N_{eq}$  are free parameters that were adjusted to minimize the mean squared error between the data and the fit. Equivalent intrinsic noise ( $N_{eq}$ ) is given directly by Equation 2 and sampling efficiency ( $J$ ) is reciprocally related to  $k$  of Equation 2 according to the relationship:

$$J = (d'_c)^2 / k \tag{3}$$

where  $d'_c$  is the criterion level of detectability, which was 1.29 in the present study.<sup>23</sup>

Figure 2 illustrates the shape of the function given by Equation 2 on log-log coordinates. At low levels of  $N$  relative to  $N_{eq}$ ,  $\log E_t$  is independent of  $\log N$  and the slope of the function is 0. When  $N$  is substantially greater than the  $N_{eq}$ ,  $\log E_t$  increases in proportion to  $\log N$ . The dashed curve in Figure 2 represents the effect of a 4-fold elevation in  $N_{eq}$  relative to the

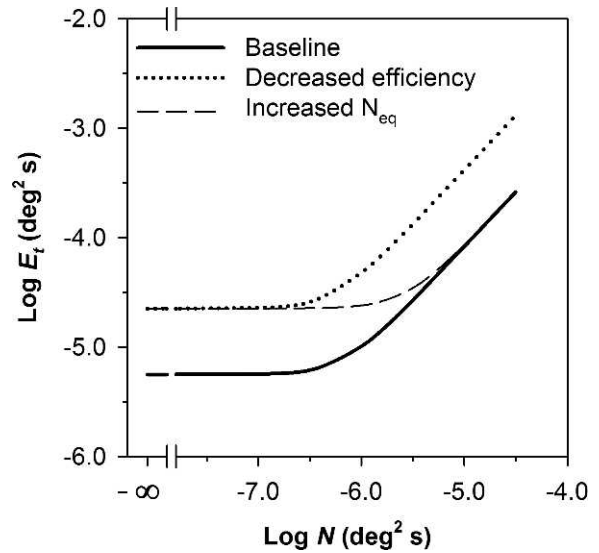


FIGURE 2. Functions generated by the LAM showing a baseline (solid line), a 4-fold elevation in  $N_{eq}$  (dashed line), and a 4-fold reduction in sampling efficiency (dotted line).

baseline (solid curve). The increase in  $N_{eq}$  shifts the curve upward and to the right by equal amounts, so that  $\log E_t$  is elevated for low values of  $\log N$ , but there is no elevation of  $\log E_t$  for high values of  $\log N$ . The dotted curve in Figure 2 represents a 4-fold reduction in efficiency. The decrease in efficiency shifts the curve uniformly upward, so that  $\log E_t$  is elevated equally for all values of  $\log N$ .

**RESULTS**

Figure 3 presents  $\log E_t$  as a function of  $\log N$  for the 10 control subjects. The log CS equivalents of the  $\log E_t$  values are shown on the right y-axis. The curves represent the least-squares best fit of Equation 2 to each subject's data. These functions provided a good fit (the mean and standard deviation of the  $R^2$

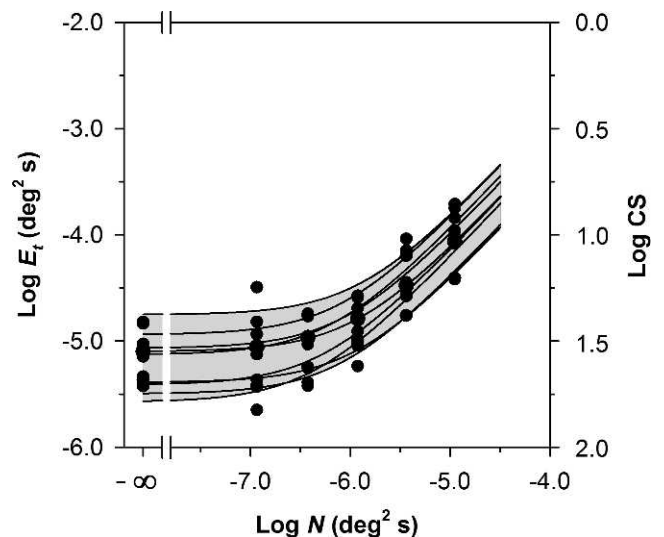


FIGURE 3.  $\log E_t$  as a function of  $\log N$  for the 10 normally-sighted control subjects. The log CS equivalents of the  $\log E_t$  values are given on the right y-axis. The curves represent the least-squares best fits of Equation 2 to the data of each individual control subject. The gray region represents the normal range, as defined in the text.

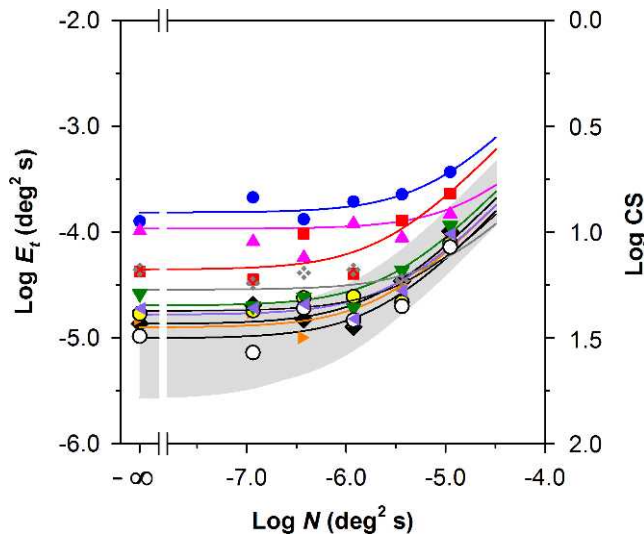


FIGURE 4.  $\log E_t$  as a function of  $\log N$  for the 10 patients with RP compared with the normal range for the 10 control subjects (gray region). The  $\log CS$  equivalents of the  $\log E_t$  values are given on the right y-axis. The curves represent the least-squares best fits of Equation 2 to the data of each patient with RP, with symbols corresponding to those shown in the Table.

values for the 10 control subjects were 0.93 and 0.05, respectively). The functions showed approximately uniform vertical shifts, which correspond primarily to differences in sampling efficiency among the control subjects (cf. the dotted curve in Fig. 2). The gray region, which represents the range of normal, was derived by first determining the maximum and minimum values of  $E_t$  for each value of  $N$  for the 10 control subjects. The data that define the maximum and minimum values were then fit with Equation 2 to generate the range of normal shown in Figure 3.

Figure 4 presents  $\log E_t$  as a function of  $\log N$  for the 10 patients compared with the range of normal (gray region), which is replotted from Figure 3. The symbols representing the individual patients correspond to those given in the Table. The curves are the least-squares best fits of Equation 2 to the data for the individual RP patients. These functions provided a good fit to the data (the mean and standard deviation of the  $R^2$  values for the RP patients were 0.78 and 0.14, respectively). The values of  $E_t$  measured in the absence of noise (i.e.,  $E_{t_0}$ , corresponding to the leftmost points in Fig. 4) were above the upper limit of normal for seven patients. However, only two patients had values of  $E_t$  measured in the highest level of noise (i.e., rightmost points in Fig. 4) that were above normal. Thus, the functions for the patients tended to converge at the highest noise level. Qualitatively, the pattern of results for the patients is most similar to elevated  $N_{eq}$  (cf. the dashed curve in Fig. 2).

To confirm this qualitative assessment, the values of  $N_{eq}$  and efficiency that were derived from the LAM were plotted as a function of  $E_{t_0}$  in Figures 5 and 6, respectively. Figure 5 shows  $\log N_{eq}$  versus  $\log E_{t_0}$  for the 10 patients and 10 control subjects. The upper x-axis gives the  $\log CS_0$  equivalents of the  $\log E_{t_0}$  values. The vertical and horizontal gray regions demarcate the normal range of  $\log E_{t_0}$  and  $\log N_{eq}$ , respectively. Two patients had  $\log E_{t_0}$  values (and  $\log CS_0$  values) that were within the range of normal. The remaining eight patients had values of  $\log E_{t_0}$  that were elevated by as much as 0.92 log units (approximately a factor of 8) above the upper limit of normal, corresponding to reductions of  $CS_0$  by as much as approximately a factor of 3. The values of  $\log N_{eq}$  were above the range of normal for all 10 patients, and there was a statistically

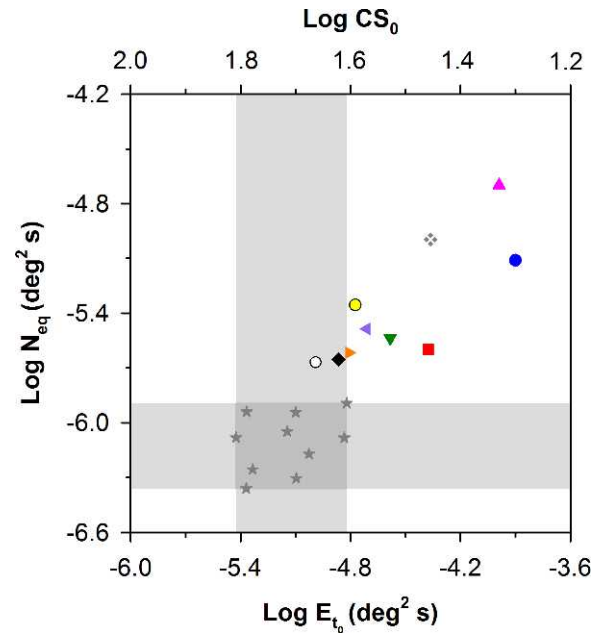


FIGURE 5.  $\log N_{eq}$  versus  $\log E_{t_0}$  for the 10 patients with RP and 10 control subjects (stars), with patient symbols corresponding to those of the Table. The gray regions demarcate the normal ranges of  $\log N_{eq}$  (horizontal region) and  $E_{t_0}$  (vertical region). The  $\log CS_0$  equivalents (i.e., CS in the absence of noise) of the  $\log E_{t_0}$  values are given on the top x-axis.

significant difference in  $\log N_{eq}$  between the patients and controls ( $t = -6.32$ ,  $P < 0.05$ ).  $\log N_{eq}$  and  $\log E_{t_0}$  were correlated significantly for the RP patients ( $r = -0.80$ ,  $P < 0.05$ ), but not for the control subjects ( $r = 0.34$ ,  $P = 0.34$ ). This

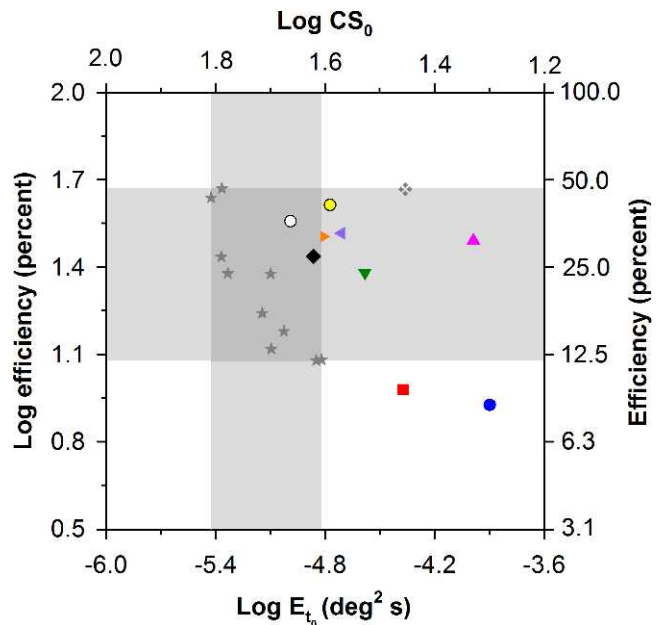


FIGURE 6. Log sampling efficiency versus  $\log E_{t_0}$  for the 10 patients with RP and the 10 control subjects (stars), with patient symbols corresponding to those of the Table. The gray regions demarcate the normal ranges of log efficiency (horizontal region) and  $E_{t_0}$  (vertical region). The  $\log CS_0$  equivalents (i.e., CS in the absence of noise) of the  $\log E_{t_0}$  values are given on the top x-axis; the linear values corresponding to log efficiency are given on the right y-axis.



is consistent with the observation that the individual functions for the patients with RP shown in Figure 4 were shifted primarily upward and rightward by equal amounts, whereas this was not the case for the control subjects (Fig. 3). There was also a statistically significant correlation between  $\log N_{eq}$  and visual field diameter ( $r = -0.69$ ,  $P < 0.05$ ), such that patients with more restricted fields, representing greater disease progression, had higher values of  $\log N_{eq}$ .

Figure 6 plots log efficiency as a function of  $\log E_{t_0}$  for the 10 patients and 10 control subjects. The vertical and horizontal gray regions demarcate the normal ranges of  $E_{t_0}$  and sampling efficiency, respectively. The efficiency values for all but two of the patients fell within the normal range, and the efficiency reductions in these two patients (nos. 8 and 9) were less than 4% below the lower range of normal. These two patients also had elevated values of  $E_{t_0}$  (0.92 and 0.45 log units above the upper limit of normal, respectively), as well as reduced visual acuity and highly constricted visual fields (Table). Two other patients (nos. 5 and 10) had relatively large elevations in  $\log E_{t_0}$ , but log efficiency that was within the normal range. These two patients also had poor visual acuity (Table). Mean log efficiency for the patients was not significantly different from that of the controls ( $t = -0.82$ ,  $P = 0.42$ ). There was no significant correlation between log efficiency and  $\log E_{t_0}$  for the patients ( $r = 0.54$ ,  $P = 0.11$ ), but the correlation was statistically significant for the controls ( $r = 0.77$ ,  $P < 0.05$ ). The significant correlation for the control subjects is consistent with the overall upward shifts of their functions shown in Figure 3.

## DISCUSSION

It has been proposed that most retinal diseases impair contrast sensitivity by increasing the level of noise within the visual pathway rather than by reducing sampling efficiency.<sup>12</sup> This study evaluated this proposal in patients with RP by measuring CS,  $N_{eq}$ , and sampling efficiency in these patients. All RP patients in our sample had a value of  $N_{eq}$  that was greater than normal, but sampling efficiency was generally within normal limits. This pattern of elevated  $N_{eq}$  with normal sampling efficiency produces a CS reduction in the absence of external noise, but normal CS in the presence of a high level of external noise. The findings of elevated  $N_{eq}$  with normal sampling efficiency suggest that high levels of noise within the visual system may, at least in part, limit CS in patients with RP, in agreement with a previous proposal.<sup>12</sup>

Although the source of the above-normal  $N_{eq}$  is presently uncertain, there are a number of potential explanations. For example, elevated  $N_{eq}$  in our patients with RP could be due to cell death, dysfunction, or the retinal remodeling that has been demonstrated in patients with retinal degenerative disease and in animal models of retinal degeneration.<sup>24</sup> Increases in  $N_{eq}$  could also be related to inner retina dysfunction (e.g., abnormal ganglion cell function due to a loss of photoreceptor input), an intriguing possibility in light of recent evidence for ganglion cell hyperactivity in rd1 and rd10 mouse models of retinal degeneration.<sup>25</sup> However, the relative contribution of these potential sources of noise to  $N_{eq}$  elevations in patients with RP requires further investigation.

Elevations in  $N_{eq}$  are typically thought to reflect increased levels of neural noise within the visual system. Nevertheless, elevated values of  $N_{eq}$  have been reported in patients with optical defects due to cataracts<sup>13,26</sup> and senescent optical changes.<sup>27,28</sup> The elevated  $N_{eq}$  for patients with optical defects is due to the fact that contrast threshold is determined by the ratio of target contrast to noise contrast (i.e., the signal-to-noise ratio). Optical attenuation affects target contrast and noise

contrast equally, leaving the ratio unchanged. Thus,  $\log E_t$  for patients with optical defects is elevated only for low values of  $\log N$ , similar to the pattern for RP patients (as shown in Fig. 4). However, it seems unlikely that optical defects would account for the elevated levels of  $N_{eq}$  in our patients with RP. These patients had minimal or no cataract, were optically corrected to minimize low-order aberrations, and viewed the stimuli through a 3-mm artificial pupil that minimized both low- and high-order aberrations. Therefore, it seems more likely that the higher levels of  $N_{eq}$  observed in our patients with RP are related to neural rather than to optical sources.

The present study measured CS in the presence of asynchronous dynamic noise, which has been shown previously to bias visual processing toward the parvocellular (PC) visual pathway.<sup>19</sup> The use of static noise, on the other hand (whether synchronous or asynchronous), appears to bias visual processing toward the magnocellular (MC) visual pathway.<sup>19</sup> However, it is unlikely that the use of a noise paradigm that biased processing toward the MC pathway would significantly alter the conclusions of the present study. Previous work has shown that the CS deficits of patients with RP are similar for conditions that are biased toward the MC or the PC pathway when measured with grating targets.<sup>7</sup> Nevertheless, it would be worthwhile to verify this conclusion by using temporal sequences of target and noise presentation and forms of luminance noise that are designed to target either the MC or the PC pathway in patients with RP.

In conclusion, our results indicate that an increased level of intrinsic noise within the visual pathway is a major determinant of CS impairments in RP patients, but even patients with normal CS can have increased equivalent intrinsic noise. Thus, CS measurement in both the presence and absence of luminance noise can provide important information about visual dysfunction in patients with RP that cannot be obtained from noise-free CS measurements alone. Furthermore, CS measurements made in the presence and absence of external noise might be of use as an outcome measure in future treatment trials and for assessing macular dysfunction in patients with RP.

## Acknowledgments

Supported by National Institutes of Health Research Grants R00EY019510 (JJM) and R01EY008301 (KRA); Core Grant P30EY001792; a Center Grant from the Foundation Fighting Blindness (GAF); the Grant Healthcare Foundation (GAF); the Pangere Corporation (GAF); and an unrestricted departmental grant from Research to Prevent Blindness.

Disclosure: **J.J. McAnany**, None; **K.R. Alexander**, None; **M.A. Genead**, None; **G.A. Fishman**, None

## References

- Berson EL. Retinitis pigmentosa. The Friedenwald Lecture. *Invest Ophthalmol Vis Sci*. 1993;34:1659-1676.
- Fishman GA. Retinitis pigmentosa. Visual loss. *Arch Ophthalmol*. 1978;96:1185-1188.
- Marmor MF. Visual loss in retinitis pigmentosa. *Am J Ophthalmol*. 1980;89:692-698.
- Grover S, Fishman GA, Alexander KR, Anderson RJ, Derlacki DJ. Visual acuity impairment in patients with retinitis pigmentosa. *Ophthalmology*. 1996;103:1593-1600.
- Lindberg CR, Fishman GA, Anderson RJ, Vasquez V. Contrast sensitivity in retinitis pigmentosa. *Br J Ophthalmol*. 1981;65:855-858.
- Sucs FE. Alteration of the light thresholds in scotopic and photopic vision in retinitis pigmentosa. *Ophthalmic Paediatr Genet*. 1984;4:171-176.

7. Alexander KR, Barnes CS, Fishman GA, Pokorny J, Smith VC. Contrast sensitivity deficits in inferred magnocellular and parvocellular pathways in retinitis pigmentosa. *Invest Ophthalmol Vis Sci.* 2004;45:4510-4519.
8. Alexander KR, Derlacki DJ, Fishman GA. Visual acuity vs letter contrast sensitivity in retinitis pigmentosa. *Vision Res.* 1995; 35:1495-1499.
9. Alexander KR, Derlacki DJ, Fishman GA. Coherence and the judgment of spatial displacements in retinitis pigmentosa. *Vision Res.* 1999;39:2267-2274.
10. Alexander KR, Derlacki DJ, Fishman GA, Szlyk JP. Grating, vernier, and letter acuity in retinitis pigmentosa. *Invest Ophthalmol Vis Sci.* 1992;33:3400-3406.
11. Alexander KR, Derlacki DJ, Xie W, Fishman GA, Szlyk JP. Discrimination of spatial displacements by patients with retinitis pigmentosa. *Vision Res.* 1998;38:1171-1181.
12. Pelli DG, Levi DM, Chung ST. Using visual noise to characterize amblyopic letter identification. *J Vis.* 2004;4:904-920.
13. Kersten D, Hess RF, Plant GT. Assessing contrast sensitivity behind cloudy media. *Clin Vis Sci.* 1988;2:143-158.
14. Pelli DG, Farell B. Why use noise? *J Opt Soc Am A.* 1999;16: 647-653.
15. McAnany JJ, Alexander KR. Spatial contrast sensitivity in dynamic and static additive luminance noise. *Vision Res.* 2010; 50:1957-1965.
16. Brainard D. The psychophysics toolbox. *Spat Vis.* 1997;10: 433-436.
17. McAnany JJ, Alexander KR. Contrast sensitivity for letter optotypes vs. gratings under conditions biased toward parvocellular and magnocellular pathways. *Vision Res.* 2006; 46:1574-1584.
18. Legge GE, Kersten D, Burgess AE. Contrast discrimination in noise. *J Opt Soc Am A.* 1987;4:391-404.
19. McAnany JJ, Alexander KR. Contrast thresholds in additive luminance noise: effect of noise temporal characteristics. *Vision Res.* 2009;49:1389-1396.
20. Manahilov V, Calvert J, Simpson WA. Temporal properties of the visual responses to luminance and contrast modulated noise. *Vis Res.* 2003;43:1855-1867.
21. Lu ZL, Doshier BA. Characterizing human perceptual inefficiencies with equivalent internal noise. *J Opt Soc Am A.* 1999; 16:764-778.
22. Watson AB, Pelli DG. QUEST: a Bayesian adaptive psychometric method. *Percept Psychophys.* 1983;33:113-120.
23. Green DM, Swets JA. *Signal Detection Theory and Psychophysics.* New York: John Wiley & Sons; 1966.
24. Marc RE, Jones BW, Watt CB, Strettoi E. Neural remodeling in retinal degeneration. *Prog Retin Eye Res.* 2003;22:607-655.
25. Stasheff SE, Shankar M, Andrews MP. Developmental time course distinguishes changes in spontaneous and light-evoked retinal ganglion cell activity in rd1 and rd10 mice. *J Neurophysiol.* 2011;105:3002-3009.
26. Pardhan S, Gilchrist J, Beh GK. Contrast detection in noise: a new method for assessing the visual function in cataract. *Optom Vis Sci.* 1993;70:914-922.
27. Pardhan S, Gilchrist J, Elliott DB, Beh GK. A comparison of sampling efficiency and internal noise level in young and old subjects. *Vision Res.* 1996;36:1641-1648.
28. Bennett PJ, Sekuler AB, Ozin L. Effects of aging on calculation efficiency and equivalent noise. *J Opt Soc Am A.* 1999;16:654-668.